Torus breakdown in a two-stroke relaxation memristor

Jean-Marc Ginoux, Riccardo Meucci, Stefano Euzzor, Angelo Di Garbo

Version of Record: https://www.sciencedirect.com/science/article/pii/S0960077921009486
Manuscript_8225648588b15acc4b9913150a8607e8

TORUS BREAKDOWN IN A TWO-STROKE RELAXATION MEMRISTOR

Jean-Marc GINOUX[a*], Riccardo MEUCCI[b] Stefano EUZZOR[b*] & Angelo DI GARBO[c]
[a] *Aix Marseille Univ, Université de Toulon, CNRS, CPT, Marseille, France, ginoux@univ-tln.fr,*
[b] *Istituto Nazionale di Ottica, Consiglio Nazionale delle Ricerche, Largo E. Fermi 6, 50125 Firenze, Italy,*
[c] *Istituto di Biofisica, Consiglio Nazionale delle Ricerche, Via G. Moruzzi 1, 56124 Pisa, Italy.*

Experimental study of a *two-stroke relaxation oscillator* (TSO) has enabled to show that this electronic component has the same features as the so-called "memristor". So, we have used the memristor's direct current (DC) $v_M - i_M$ characteristic for modeling the TSO's DC current-voltage characteristic. This led us to confirm on one hand, that the TSO is a memristor and, on the other hand to propose a new four-dimensional autonomous dynamical system allowing to describe experimentally observed phenomena such as the transition from a limit cycle to torus breakdown.

I. FROM TWO-STROKE OSCILLATOR TO TWO-STROKE MEMRISTOR

A. The Two-Stroke Relaxation Oscillator

In the beginning of the sixties, the French engineer, mathematician and physicist Philippe Le Corbeiller (for more details about his works and life, see Ginoux [1]) initiated the study of *TSOs*. He considered "several mathematical models of non-symmetrical oscillators, in which the energy stored in the generalized flywheel varies from a minimum to a maximum value and back again *only once per period*." He called these oscillators *TSOs* [2] and provided the following general *nonlinear ordinary differential equation* characterizing their oscillations:

$$\ddot{x} + F\left(\dot{x}\right) + x = 0. \tag{1}$$

He named it *Lord Rayleigh-type equation* (LRT) in reference to the works Sir William Strutt, alias, Lord Rayleigh [3] on maintained vibrations and explained that the *characteristic function* $F(\dot{x})$ is such that the equation (1) has a unique periodic solution, i.e., a Poincaré's *limit cycle* [4, p. 261]. In fact, as recalled by Ginoux [1], this *characteristic function* $F(\dot{x})$ plays the role of a "negative resistance" the sign of which is alternating between positive and negative values such that the oscillations are self-sustained instead of being damped. Of course, the main difficulty in this problem lies in the modeling of such *characteristic function*. In his paper, Le Corbeiller [2] wrote that he "has tried out a number of functions, some with one, and some with two exponentials, which lead to two-stroke oscillators."

Less than ten years after, the American electronics scientist Donald L. Hester [5] published an article in which he showed that simplified versions of tuned-collector, tuned-base, and Hartley transistor oscillators are characterized by a nonlinear ordinary differential equation of the form:

$$\ddot{x} - \mu\left[e^{a\dot{x}} - \kappa e^{(a+b)\dot{x}}\right] + \gamma\dot{x} + x = 0, \tag{2}$$

where μ, κ, γ, a and b are positive constants and $\kappa \ll 1$. Hester [5] used the Ebers-Moll large-signal model for bipolar junction transistors [6]. So, the *characteristic function* of his LRT equation (2) read:

$$F\left(\dot{x}\right) = -\mu\left[e^{a\dot{x}} - \kappa e^{(a+b)\dot{x}}\right] + \gamma\dot{x} = -f\left(\dot{x}\right) + \gamma\dot{x}. \tag{3}$$

While using the classical D'Alembert transformation [7], Hester's LRT equation (2) can be recast in its most general form as a two-dimensional dynamical system:

$$\begin{cases} \dfrac{dx}{dt} = -y, \\ \dfrac{dy}{dt} = x + F\left(\dot{x}\right) = x - \gamma y - f\left(-y\right). \end{cases} \tag{4}$$

Following these seminal works and by setting $\gamma = 0$ in Eq. (4), Jelbart and Wechselberger [8] recently proposed a model for the electronic *two-stroke oscillator* which can be written as follows:

$$\begin{cases} \dfrac{dx}{dt} = -y, \\ \dfrac{dy}{dt} = x - R\left(y\right), \end{cases} \tag{5}$$

where x and y denotes respectively dimensionless 'current' and 'voltage' and

$$R(y) = f(-y) = \mu \left[e^{-ay} - \kappa e^{-(a+b)y} \right]. \tag{6}$$

The intersection of the nullclines of Eq. (5) defines the fixed points of the corresponding dynamical system. Moreover, the nullcline corresponding to the equation describing the time evolution of $y(t)$ can be employed to define the *characteristic function* of the *two-stroke oscillator*: $x = R(y) = f(-y)$ that has been plotted in Fig. 1 with the parameter values given in [8], i.e. for $(\mu,\, \kappa,\, a,\, b) = (1,\, 10^{-2},\, 4,\, 6)$.

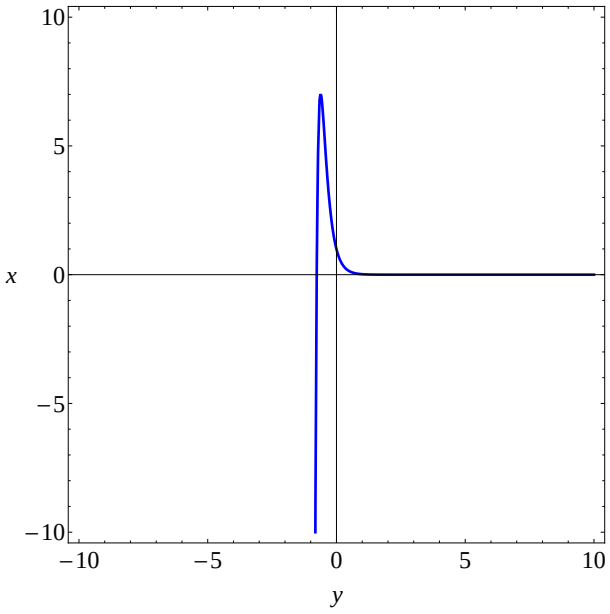

FIG. 1: *Characteristic function* of the *two-stroke oscillator* (6).

B. The memristor

The missing two terminal circuit element,that is, the memristor, postulated fifty years ago by L.O. Chua was finally implemented in 2008 [9]. However, contrary to what one might think, it is not by experimenting, but by logical deduction that L. O. Chua was able to postulate the existence of a missing circuit element. In particular, in his now famous publication of 1971, L.O. Chua [10] considered the three basic building blocks of an electric circuit: the capacitor, the resistor and the inductor as well as the three laws linking the four fundamental circuit variables, namely, the electric *current* i, the *voltage* v, the *charge* q and the *magnetic flux* φ (see Fig. 2). Then, L.O. Chua [10, p. 507] explained that:

> "... by the *axiomatic* definition of the three classical circuits elements, namely, the *resistor* (defined by a relationship between v and i), the *inductor* (defined by a relationship between φ and i), and the *capacitor* (defined by a relationship between q and v). Only one relationship remains undefined, the relationship between φ and q."

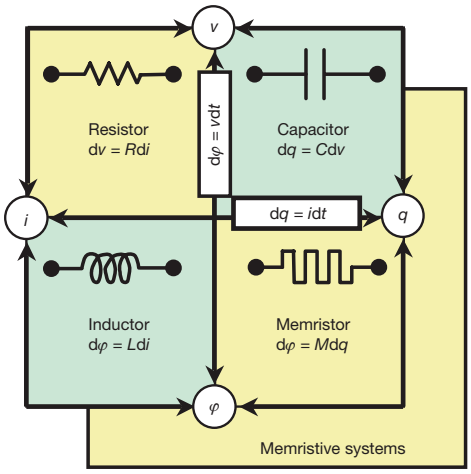

FIG. 2: The four fundamental two-terminal circuit elements, [9, p. 80]

He thus concluded from the logical as well as axiomatic points of view, that it is necessary, for the sake of *completeness*, to postulate the existence of a fourth circuit element to which he gave the name *memristor* since it behaves like a nonlinear resistor with memory [11]. Unlike the transistor that allows the current to flow or not, and so uses bits (0 or 1), the memristor has a variable resistance and can therefore take all the values between 0 and 1. Depending on the incoming signal and its previous state, the memristor adjusts its resistance to current and keep in memory its previous state, hence its name. In 2010, Muthuswamy & Chua [12, p. 1574] plotted the direct current (DC) $v_M - i_M$ *characteristic function* of the memristor (see Fig. 3).

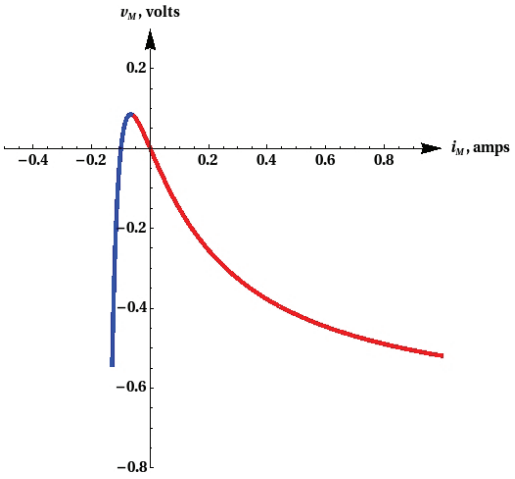

FIG. 3: The DC $v_M - i_M$ *characteristic function* of the memristor, [12, p. 1574].

In their paper, Muthuswamy & Chua [12, p. 1580] stated the equation of this curve representing the direct current (DC) $v_M - i_M$ *characteristic function* of the memristor:

$$v_M = i_M \left(-1 + \frac{i_M^2}{(i_M + \alpha)^2} \right) \beta. \tag{7}$$

The comparison of the graphs reported in figures 1 and 3 clearly show that, apart for the meaning of the variables, translations and scale factors, they exhibit a similar dependence on the independent variables. Thus, the great similarity between the shape of such curves motivated us to adopt as *characteristic function* of the *two-stroke oscillator* (6) a functional form corresponding to that of the *memristor* in equation (7). Consequently, according to this rationale,

we assume that the *characteristic function* $x = R(y)$ of the *two-stroke oscillator* is described by a memristor's like direct current (DC). More precisely, we define:

$$x = R\left(y\right) = g\left(y\right) = y\left(-1 + \frac{y^2}{\left(y+a\right)^2}\right)b \tag{8}$$

where a, b are parameters to be determined from the experimental data. In our laboratory we already measured the electrical nonlinear voltage-current characteristic of the UJT (Unipolar Junction Transistor; for more details see Fig. 3b in Ref.[13] where the $V_E - I_E$ characteristic is shown and Fig. 8 in section IV of this manuscript where the schematic of the UJT relaxation oscillator is represented Then, the values of the parameters a and b were determined by fitting our experimental data with the characteristic defined in Eq. 8 and the result were:

$$a = -0.0546778, \quad b = 14.0334,$$

with the coefficient of determination $R^2 = 0.929789$ indicating a quite good fit of the data [14]

C. Two-stroke relaxation memristor

Thus, starting from the previous works of Le Corbeiller [2], Hester [5] and Jelbart and Wechselberger [8] and by using the *memristor characteristic function* (8), we designed the following *two-stroke relaxation memristor* model.

$$\begin{cases} \dfrac{dx}{dt} = -y, \\ \dfrac{dy}{dt} = x - y\left(-1 + \dfrac{y^2}{\left(y+a\right)^2}\right)b, \end{cases} \tag{9}$$

where x and y denotes respectively dimensionless 'voltage' and 'current' and $a = -0.0546778$ and $b = 14.0334$. The numerical integration of this dynamical system (9) was performed and the quantities $-x$ and $-y$ are plotted in Figs. 4a & 4b.

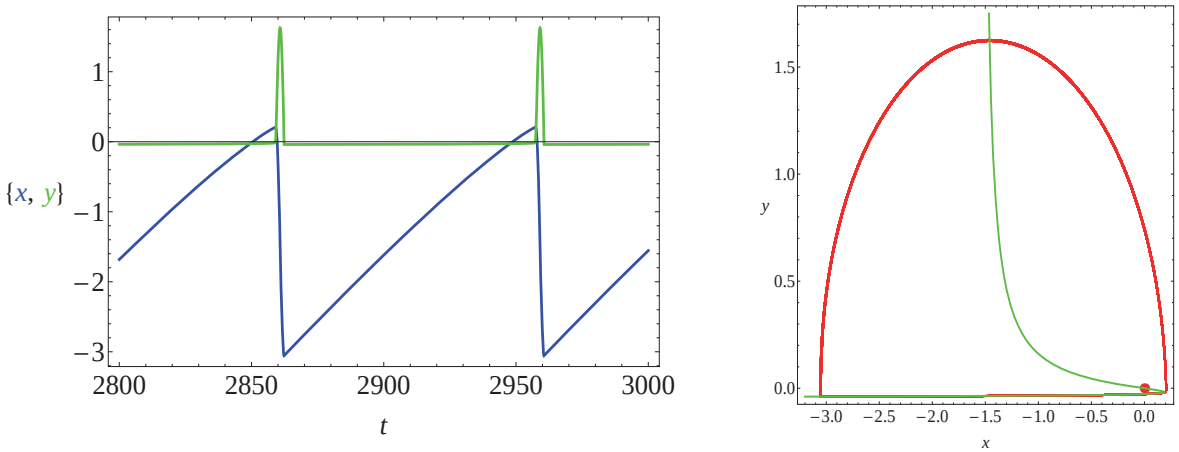

(a) Time series

(b) Phase plane

FIG. 4: *Two-stroke relaxation memristor* model (9).

It appears that we obtain exactly the same results as Hester [5] and Jelbart and Wechselberger [8].

II. CHAOTIC TWO-STROKE RELAXATION MEMRISTOR

Now we are in position to define our *two-stroke relaxation oscillator* by just performing the following transformations: a) changing symbolic representation of the dependent variables ($x \longrightarrow y$ and $y \longrightarrow x$); b) reversing signs ($x \longrightarrow -x$ and $y \longrightarrow -y$). With these changes the dynamical systems employed to define our *two-stroke relaxation oscillator* (9) reads:

$$\begin{cases} \dfrac{dx}{dt} = y - x\left(-1 + \dfrac{x^2}{(x-a)^2}\right) b = y - g\left(x\right), \\ \dfrac{dy}{dt} = -x. \end{cases} \tag{10}$$

It is worth noticing that, due to the symmetry properties of Eqs. 9, the above transformations produced only a change in the relative sign between the two terms in the denominator of the *memristor characteristic function*. The dimensionality of the above *two-stroke relaxation oscillator* model can be increased by adding an external sinusoidal driving term $\sin(\omega t)$. This makes the system non-autonomous and chaotic instabilities can be easily foreseen by adjusting the forcing term. In addition, the equation describing the voltage variable can be slightly modified by adding other two terms accounting for specific features of UJT oscillator (see [15] for additional details). Definitely, the second equation (10) is modified as it follows:

$$\frac{dy}{dt} = A_0 - A_1 y - A_2 x + \varepsilon\omega z, \tag{11}$$

where $z(t)$ is the solution of the *harmonic oscillator*, satisfying the initial conditions z(0)=0 and z(0)=1, described by the equations:

$$\begin{aligned} \frac{dz}{dt} &= u, \\ \frac{du}{dt} &= -\omega^2 z. \end{aligned} \tag{12}$$

This strategy, which represents a general way to introduce a coupling with another oscillator, was successfully applied for modeling the complex dynamics of a glow discharge Ne tube [16]. Thus, the continuous model for the UJT, i.e., for the *two-stroke relaxation memristor* can be rewritten as it follows:

$$\begin{aligned} \frac{dx}{dt} &= y - g\left(x\right), \\ \frac{dy}{dt} &= A_0 - A_1 y - A_2 x + \varepsilon\omega z, \\ \frac{dz}{dt} &= u, \\ \frac{du}{dt} &= -\omega^2 z. \end{aligned} \tag{13}$$

where: $a = -0.0546778$, $b = 14.0334$, $A_0 = 0.01$, $A_1 = 0.7925$, $A_2 = 49.59$ and $\omega = 2\pi\nu$ with $\nu = 0.2944$. The adopted values of A_0, A_1, A_2 are from [15] where they were also employed to describe another UJT model based on the analogies with the glow discharge in a Ne tube. In this relaxation oscillator it is physically plausible to introduce a parasitic inductive effect while for the UJT oscillator, this effect has been introduced as an "ad hoc" one to have two separate time scales.

III. STABILITY ANALYSIS

A. Fixed points

Fixed points are determined while using the classical nullclines method. Thus, by plugging y and z in the first equation of the dynamical system (13) we obtain, with this parameter set, the following unique real fixed point of this four-dimensional dynamical system:

$$I\left(x^*, y^* = \frac{A_0}{A_1} - \frac{A_2}{A_1}x^*, z^* = 0, u^* = 0\right), \tag{14}$$

where the expression of x^* (too large to be explicitly written here) only depends A_0 and A_2 and not on the control parameter ε. Moreover, with this parameter set, $x^* \ll 1$ ($x^* \approx 0.0002599$). So, this fixed point is very near the origin.

B. Jacobian matrix

The Jacobian matrix of dynamical system (13) reads:

$$J = \begin{pmatrix} -g'(x) & 1 & 0 & 0 \\ -A_2 & -A_1 & \varepsilon\omega & 0 \\ 0 & 0 & 0 & 1 \\ 0 & 0 & -\omega^2 & 0 \end{pmatrix} \tag{15}$$

where
$$g'(x) = -\frac{a^2 b(a-3x)}{(a-x)^3} \tag{16}$$

By replacing the coordinate of the fixed point I (14) in the Jacobian matrix (15) one obtains the following Cayley-Hamilton fourth degree eigenpolynomial:

$$\left(\lambda^2 + \omega^2\right)\left[\lambda^2 + (A_1 + g'(x))\,\lambda + A_2 + A_1 g'(x)\right] = 0. \tag{17}$$

Thus, it appears that the eigenpolynomial (17) has a pair of two complex conjugate eigenvalues $\lambda_{1,2} = \pm i\omega$ which correspond to those of the *harmonic oscillator* and a pair of real eigenvalues:

$$\lambda_{3,4} = \frac{1}{2}\left[-(A_1 + g'(x)) \pm \sqrt{\Delta}\right] \tag{18}$$

where
$$\Delta = (A_1 - g'(x))^2 - 4A_2 \tag{19}$$

Since, with this parameter set $x^* \ll 1$, we have according to (16): $g'(x^*) \approx -b$. So, $\Delta > 0$ and the real parts of all eigenvalues are strictly positive $(8.93398, 4.30595)$. So, the fixed point I is unstable according to Lyapunov's theorem [17].

C. Bifurcation diagram

From equations 13 it follows that the dynamical properties of the forced TSO strongly depend on the amplitude (ε) and frequency (ω) of the harmonic forcing. Thus, in order to highlight how the changes of these control parameters impact the corresponding dynamics of the attractor we have built a bifurcation diagram (see Fig. 5). Moreover, for a more clear identification of the possible occurring dynamical regimes we have compared the phase portraits and Poincaré section plotted in Fig. 6 & 7. Analysis of this bifurcation diagram shows that for $\varepsilon = 0$, the attractor is a *limit cycle* of period 1 (see Fig. 6a & 7a). When $0 < \varepsilon < 0.46$, the attractor becomes a "torus" and its trajectories are dense on the attractor (see Fig. 6b & 7b). For $0.46 < \varepsilon < 0.463$, the "torus" breaks down (see Fig. 6c & 7c). For $0.463 < \varepsilon < 1.77$, a limit cycle of period 2 appears. When $1.77 < \varepsilon < 1.94$ a period doubling cascade occurs and leads to a chaotic attractor (see Fig. 6d & 7d). Finally, for $1.94 < \varepsilon < 2.05$ a reverse period doubling cascade occurs and *limit cycle* of period 2, 3 and 4 appears(see Fig. 6f & 7f). In order to confirm this scenario, Lyapunov exponents have been computed in each case.

D. Numerical computation of the Lyapunov exponents

The algorithm developed by Sandri [18] for Mathematica® has been used to perform the numerical calculation of the Lyapunov characteristics exponents (LCE) of dynamical system (13) in each case. LCEs values have been computed within each considered interval ($\varepsilon \in [0, 0.463]$ and $[1.77, 2]$). As an example, for $\varepsilon = 0.4623, 1.92$ and 2, the corresponding LCEs are $(0, 0, -0.033, -78.53)$, $(+0.043, 0, -0.037, -85.05)$ and $(+0.042, 0, -9.26, -89.31)$, respectively. Then, following the works of Klein and Baier [19], a classification of (autonomous) continuous-time attractors of dynamical system (13) on the basis of their Lyapunov spectrum, together with their Hausdorff dimension is presented in Tab. 1. LCEs values have been also computed with the Lyapunov Exponents Toolbox (LET) developed by Siu for MatLab® and involving the two algorithms proposed by Wolf *et al.* [20] and Eckmann and Ruelle [21] (see https://fr.mathworks.com/matlabcentral/fileexchange/233-let). Results obtained by both algorithms are consistent.

TABLE I: Lyapunov characteristics exponents of dynamical system (13) for various values of ε.

ε	LCE spectrum	Dynamics of the attractor	Hausdorff dimension
$\varepsilon = 0$	$(0, -, -, -)$	Periodic Motion (Limit Cycle)	$D = 1$
$0 < \varepsilon < 0.463$	$(0, 0, -, -)$	3-Torus	$D = 2$
$1.77 < \varepsilon < 2$	$(+, 0, -, -)$	2-Chaos	$D = 3.0007$

IV. EXPERIMENTAL MEASUREMENTS

The experimental set up of the driven UJT oscillator is reported in Fig. 8. The UJT is a 2N2646 - Motorola and it is connected from the emitter side E through the resistor R (12.68 $k\Omega$) to the supply voltage V_s fixed at $7.0(V)$. The B2 base is connected to a modulated bias voltage having a dc value is fixed at $V_b = 4.8V$. The B1 base is tied to ground through a resistor R_L (56 Ω).The discharge current through the UJT is detected as a voltage signal on R_L. The capacitor C has a value of 49.73 nF. According to [22] the period T_{exp} of the "relaxation oscillator" can be approximated by the following formula:

$$T_{exp} \cong RC \log\left(\frac{1}{1 - \eta_{exp}}\right), \tag{20}$$

where η_{exp} is the "intrinsic stand off ratio", typically in the range $0.4 - 0.8$. So, by considering the frequency of our relaxation oscillator ($4742Hz$), we can deduce from (20) $\eta_{exp} \approx 0.28$. Although this experimental value is a little bit outside the expected range, we can justify it by considering that this value is obtained when V_s is set equal to V_b while in our scheme these two values are different. We will discuss at the end of this section the possibility to introduce formally a similar relationship for the TSO model.

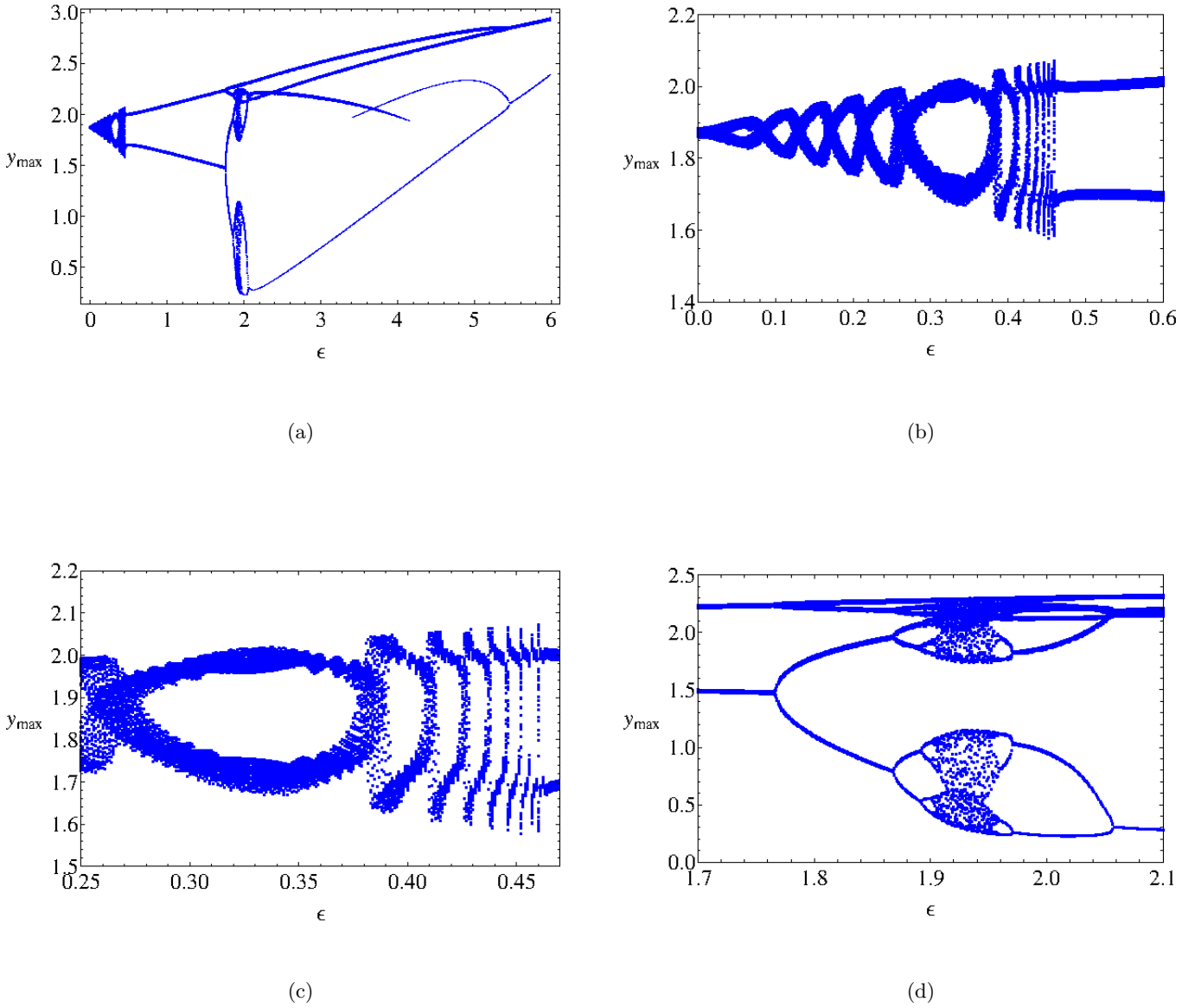

FIG. 5: Bifurcation diagram y_{max} as function of ε.

The dynamics of the UJT relaxation oscillator has been tracked in real time by the Poincaré's sections implemented on the current signal on the load resistor R_L. The apparatus for recording the Poincaré's sections include sample and hold circuits to memorize the peaks of the current signal I_n as well as the same sequence delayed by one peak I_{n-1}. The two sequences are plotted in $x-y$ configuration on a digital scope Tektronix TDS7104. The intrinsic oscillation frequency of the UJT oscillator was $\nu = 4742Hz$ and the frequency of the applied harmonic perturbation term was $f = 2271Hz$ (just detuned of one hundred Hertz below $\nu/2$). Together with the Poincaré's sections we plot the attractors in the $x-y$ plane by means of another digital scope Tektronix. The plotted variables were the current through the resistor R_L and the emitter potential V_e. To build the image of the attractors the scale sensitivities were: horizontal scale $100mV/div$; vertical scale $200mV/div$. Instead, for the Poincaré's sections the sensitivities were: horizontal scale $100mV/div$; vertical scale $200mV/div$. Overall, the corresponding measurements are condensed in Fig. 9 and Fig. 10. In the first one, we report the dynamics emerging from the free running oscillation of the UJT

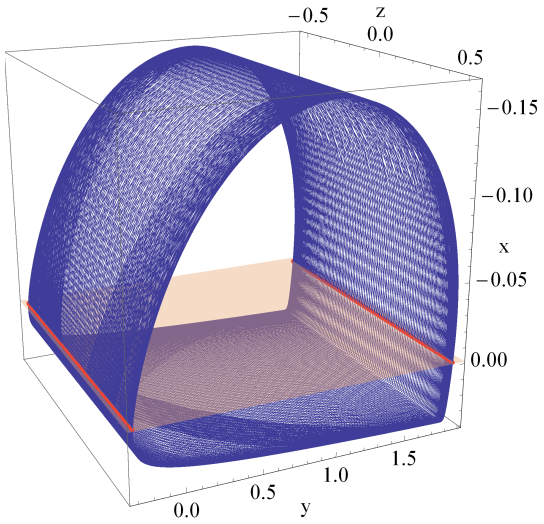

(a) $\varepsilon = 0$

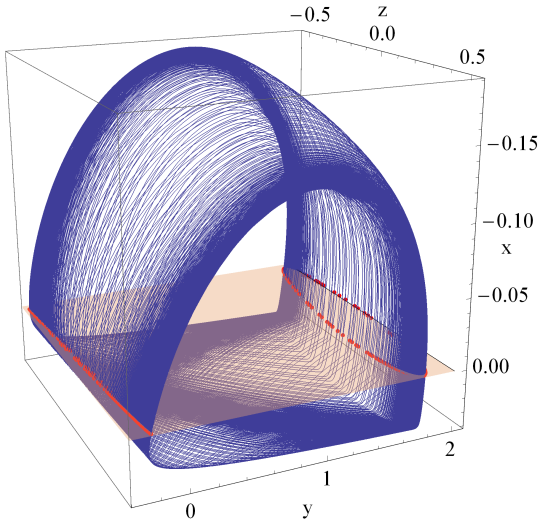

(b) $\varepsilon = 0.4$

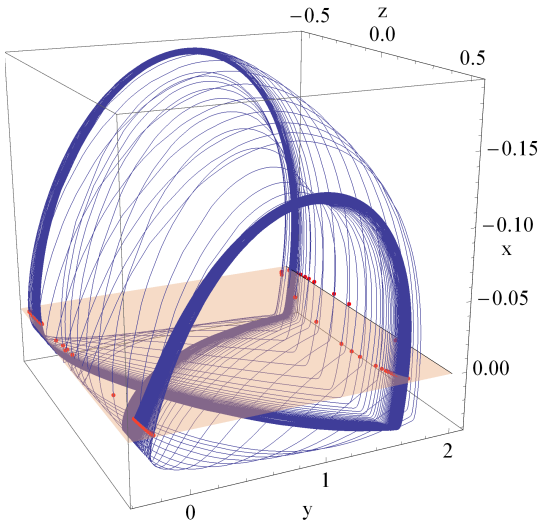

(c) $\varepsilon = 0.4623$

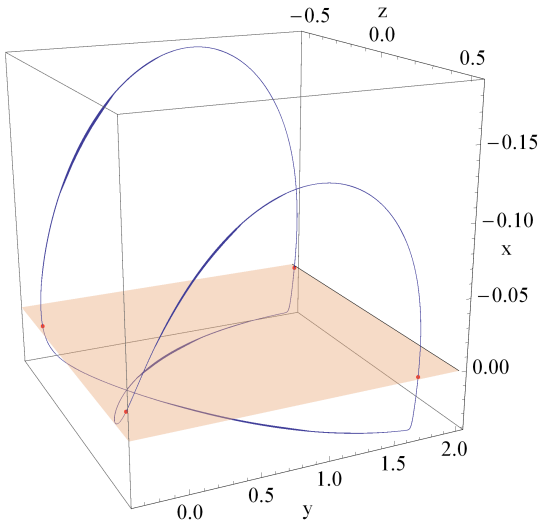

(d) $\varepsilon = 0.5$

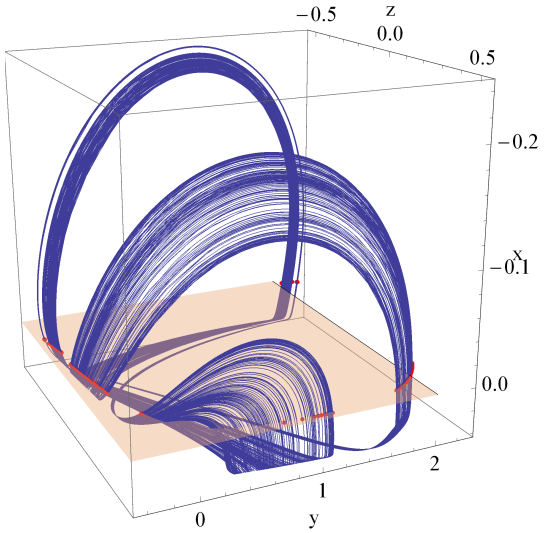

(e) $\varepsilon = 1.92$

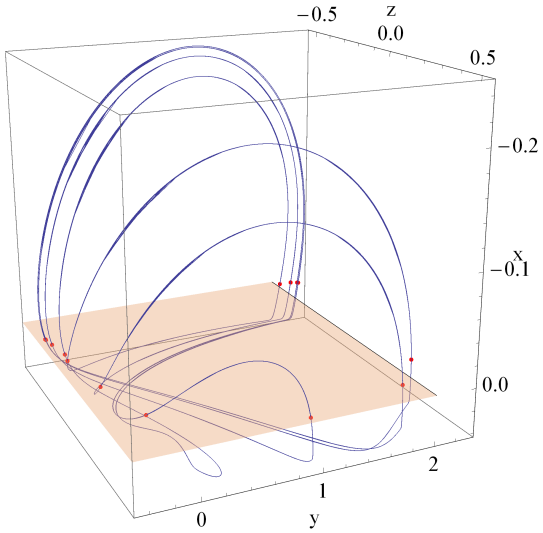

(f) $\varepsilon = 2$

FIG. 6: Poincaré section of the *chaotic two-stroke relaxation memristor* (13) in the (x, y, z)-space for various values ε.

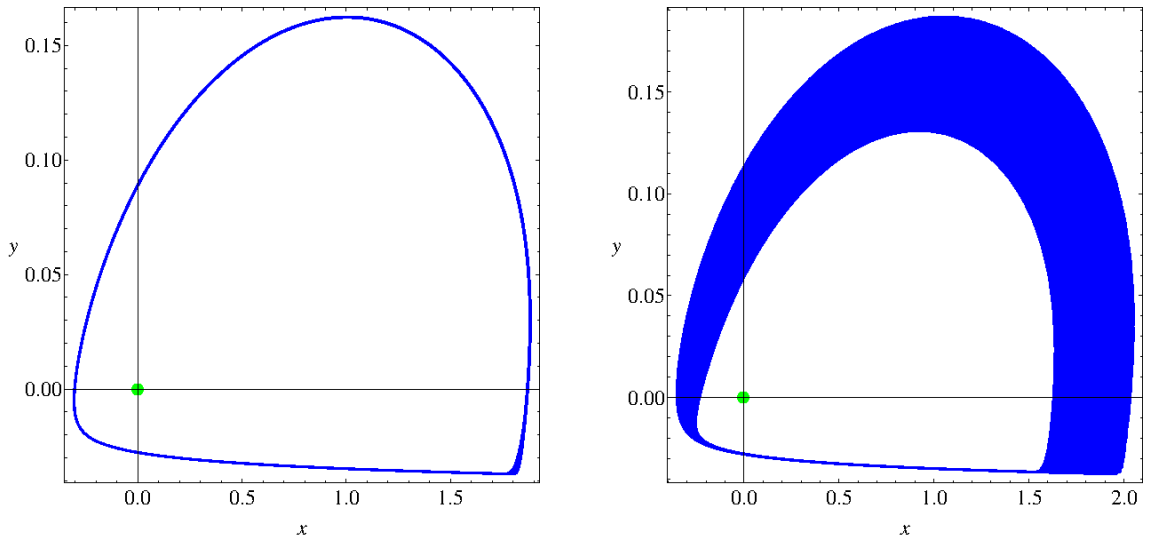

(a) $\varepsilon = 0$

(b) $\varepsilon = 0.4$

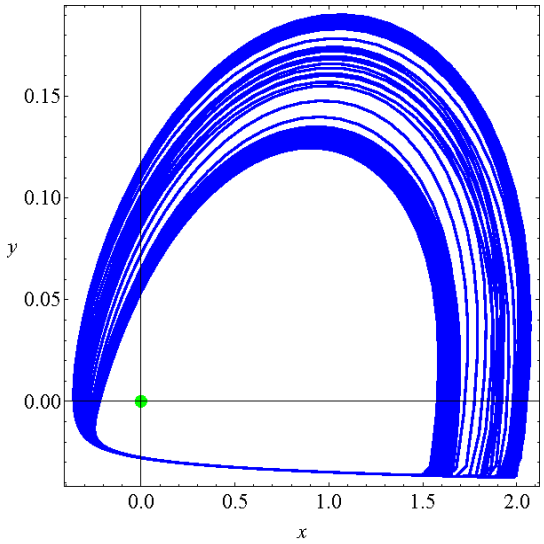

(c) $\varepsilon = 0.4623$

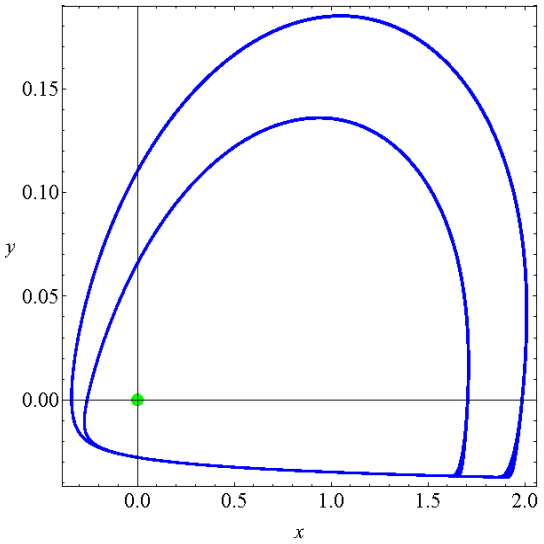

(d) $\varepsilon = 0.5$

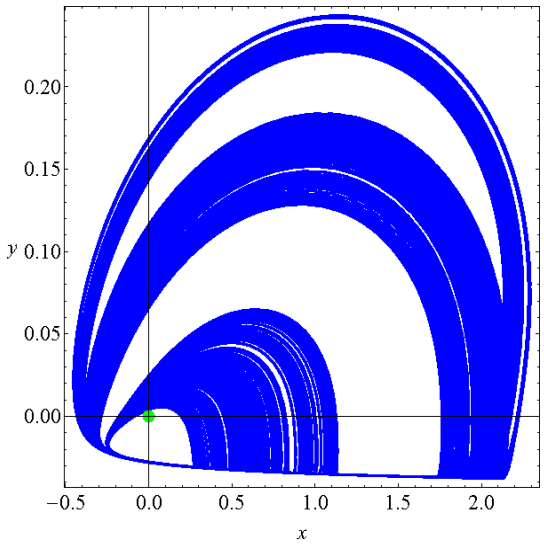

(e) $\varepsilon = 1.92$

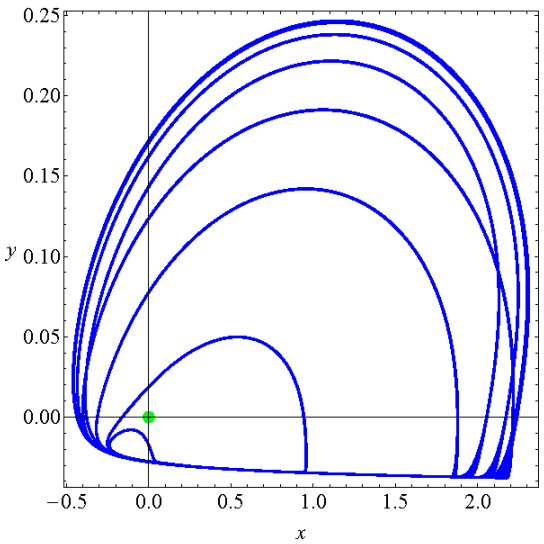

(f) $\varepsilon = 2$

FIG. 7: Phase portraits of the *chaotic two-stroke relaxation memristor* (13) in the (x, y)-plane for various values ε.

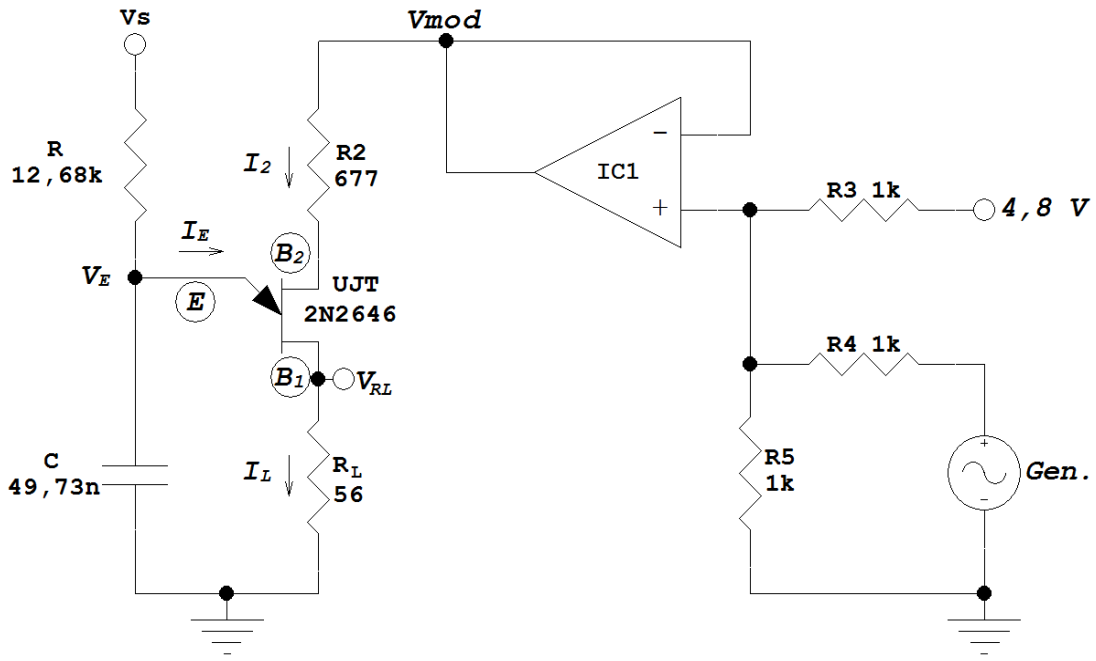

FIG. 8: Circuit diagram of the experimental setup.

oscillator (see Fig. 9a and 9b). Then, the introduction of a sinusoidal forcing at frequency near half of the free running frequency leads to a quasi-periodic regime (torus regime) characterized by closed loop Poincaré's section. As the amplitude of the perturbation is increased the torus surface enlarges and displays a folding as shown in Fig. 9c and 9d. A further increase of the driving amplitude leads to phase locking regimes where the continuity of the Poincaré's section is lost. The phase locking regimes precede the torus breaking characterized by the presence of wrinkles. This dynamical feature is the one depicted Fig. 10a and 10b. The underlying physical mechanism is competition between two frequencies, that is, the intrinsic relaxation frequency of the UJT oscillator and the driving frequency which tend to pull the intrinsic frequency towards the double of the driving frequency. This frequency pulling phenomenon is governed by the nonlinearities of the relaxation oscillator. This process is clearly evident when the amplitude of the driving term is increased (see Fig. 10c and 10d) where a chaotic period two regime is signaled by a Poincaré's section with two not well defined points. Eventually, the dynamics becomes periodic (period two solution) after a bifurcation (see Fig. 10e and 10f). A comparison with the numerical bifurcation diagram reveals that last one also shows the period doubling bifurcation sequence leading to a different chaotic regime. It is clear that this chaotic regime is more difficult to reach in the experiment where we have constraints related to the saturation of electronic components.

Figures 10 represents the torus breaking and the successive transitions to a period two solution (Scale sensitivities as in Fig.9). When the amplitude of the sinusoidal forcing term becomes equal to $800mV$, we reach the frequency locking (Fig.10a & b). Then, starting from $879mV$ the torus is breaking down (Fig. 10c & d). At $900mV$ we reach the competition regime (Fig. 10e & f). Then, a period two limit cycle appears at $1400mV$ (Fig. 10g & h).

Let us conclude this section providing an estimation of the typical value of the parameter η (here denoted η_{ty}) for the TSO model. We point out that the characteristic time scale of the UJT oscillator is given by RC [13, 22]. Therefore, a physical time scale can be introduced in the model by just rescaling the time in the TSO model according to $t' = RCt$. In this way the corresponding oscillation period of the model is given by $T_{ty} = RC1.702$, where 1.702 is the dimensionless period of this nonlinear oscillator when $\epsilon = 0$. We can formally define η_{ty} as the value satisfying the equation $T_{ty} \cong RC \log[1/(1-\eta_{ty})]$. This computation leads to $\eta_{th} \cong 0.8$ which is in agreement with the expectations.

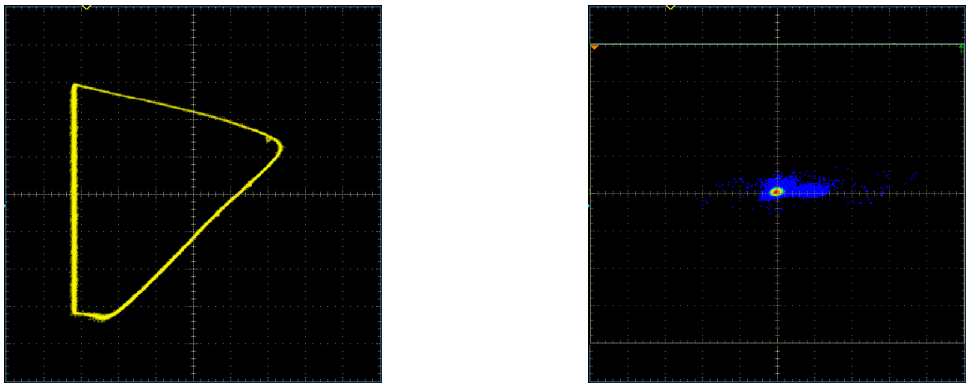

(a) $0mV$ *limit cycle* (b) $0mV$

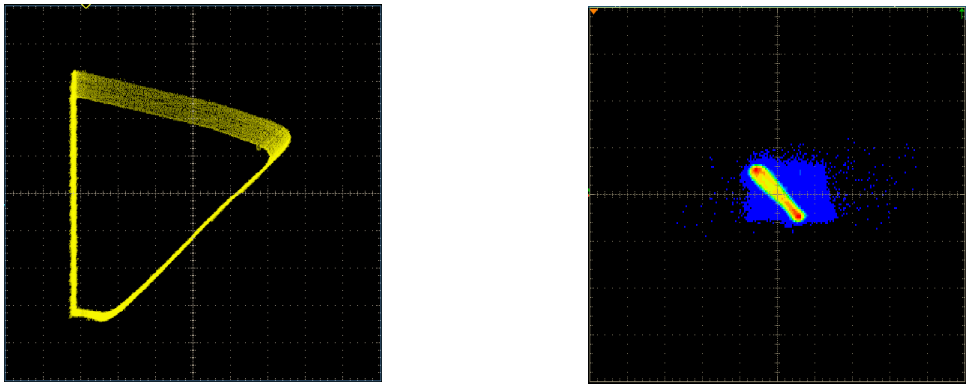

(c) $250mV$ *birth of the torus* (d) $250mV$

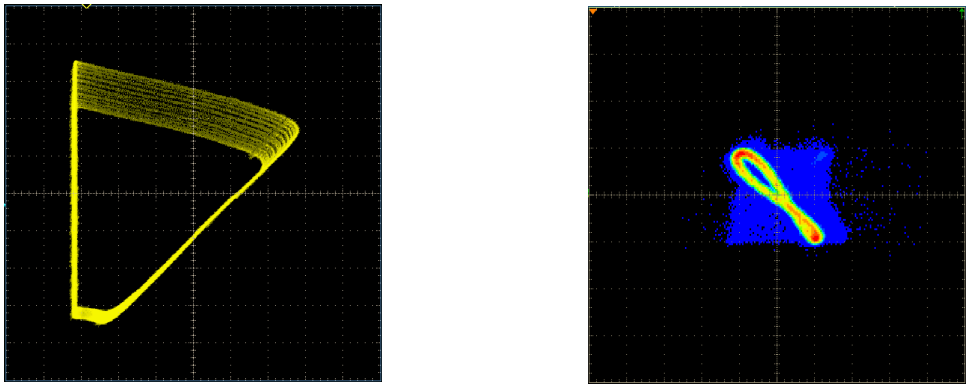

(e) $450mV$ *torus* (f) $450mV$

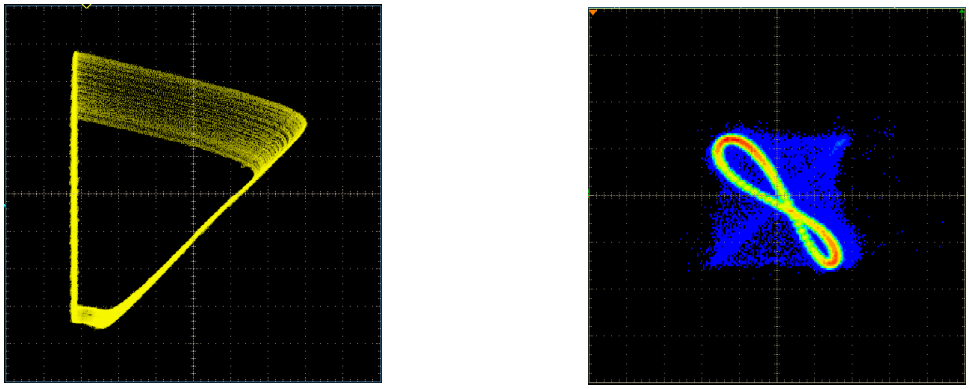

(g) $650mV$ *torus* (h) $650mV$

FIG. 9: Experimental attractors in the $x - y$ plane (left panels) and corresponding Poincaré's sections (right panels).

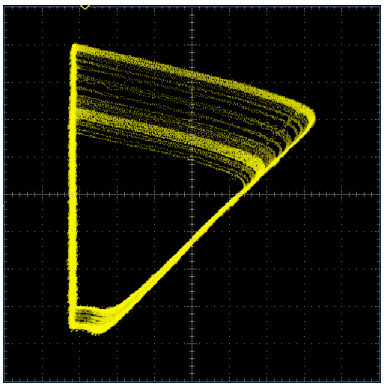

(a) $800mV$

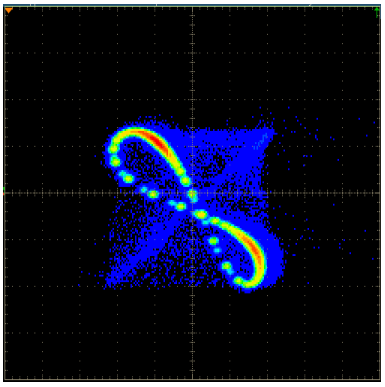

(b) $800mV$

frequency locking

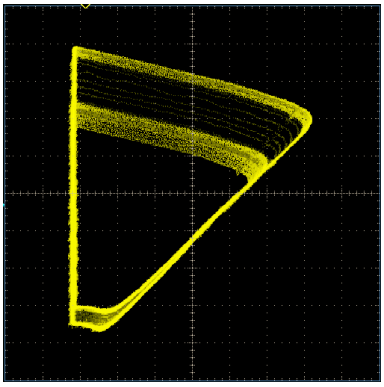

(c) $897mV$

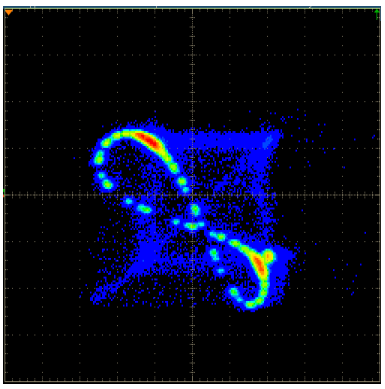

(d) $897mV$

torus breaking

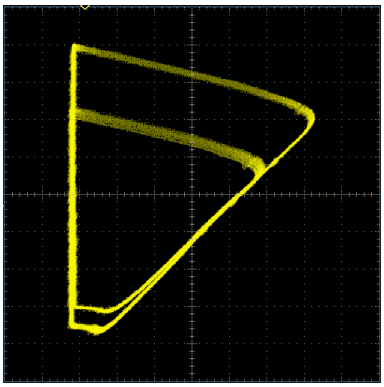

(e) $900mV$

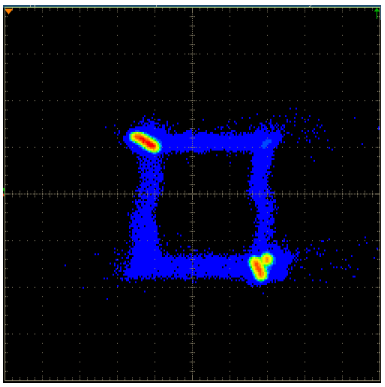

(f) $900mV$

competition regime

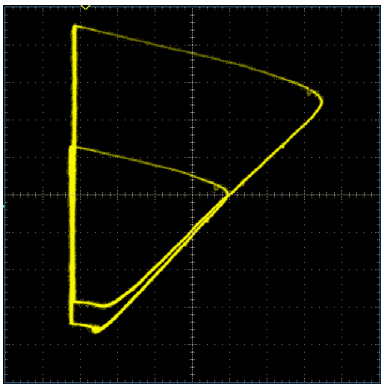

(g) $1400mV$

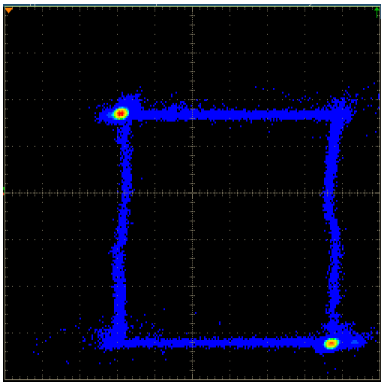

(h) $1400mV$

period two limit cycle

FIG. 10: Torus breaking and successive transitions to a period two solution.

V. CONCLUSIONS

The UJT relaxation oscillator circuit is a reliable one to generate self-sustained nonlinear oscillations and to observe the transition to chaos via quasiperiodicity(torus breakdown). Although such a system was widely studied, both experimentally and theoretically, at present we do not have a satisfactory theoretical model yet to describe its behavior. Two approaches were attempted to model it. The first one is based on the analogy with a glow discharge Ne tube. In this case, we have a continuous model resting on a parasitic inductance associated to the UJT. The second approach is based on a piece-wise linear model which accurately describes the quasiperiodic dynamics but not the transition to chaos unless a delayed term is introduced in the model. Considering the salient properties of the TSO and memristor, we propose a new continuous model able to describe the relevant features of the complex dynamics of the driven UJT oscillator.

Acknowledgments

This paper is dedicated to the memory of Prof. Tito Arecchi who passed away on 15 February 2021. Tito encouraged us to deeply investigate and revisit the concept of relaxation oscillator. One of Tito's legacies is indissolubly associated to laser instabilities with the worldwide recognized classification of laser as class A, B and C. If we restrict the attention to class B lasers ruled by two dynamical variables, that is, laser intensity and population inversion , it is quite natural to foresee at the analogies with relaxation oscillators first introduced by B. van der Pol in 1926. Also these oscillators are described by two coupled variables acting on two separate time scales. Unfortunately his departure did not allowed to share with him some recent results on these oscillators as an example the transition to chaos main and via quasi-periodicity and the analogies with the memristor, a crucial electronic component, first postulated by L.O. Chua [10], in 1971, and destined to have an increasing impact in applications.

[1] Ginoux, J. M., *History of Nonlinear Oscillations Theory*, Archimede, New Studies in the History and Philosophy of Science and Technology, vol. 49, Springer, New York, 2017.
[2] Le Corbeiller, Ph., "Two-stroke oscillators," *IRE Trans. Circuit Theory*, vol. CT-7, (December 1960) pp. 387–398.
[3] Strutt, John William, alias Lord Rayleigh, "On maintained vibrations," *Philosophical Magazine* (ser. 5) 15 (1883) pp. 229–235.
[4] Poincaré, H., "Sur les courbes définies par une équation différentielle," *Journal de mathématiques pures et appliquées*, Série III **8**, (1882) pp. 251–296.
[5] Hester, D., "The nonlinear theory of a class of transistor oscillators," *IEEE Transactions on Circuit Theory*, 15(2) (1968) pp. 111–117.
[6] Ebers, J. J. & Moll, J. L., "Large signal behavior of junction transistors," *Proc. IRE*, vol. 42 (December 1954) pp. 1761–1772.
[7] D'Alembert, J., "Suite des recherches sur le calcul intégral, quatrième partie : Méthodes pour intégrer quelques équations différentielles," *Hist. Acad. Berlin*, tome IV, (1748) pp. 275–291.
[8] Jelbart, S. & Wechselberger, M., "Two-stroke relaxation oscillators," *Nonlinearity* 33(5) (2020) pp. 2364–2408.
[9] Strukhov, D. B., Snider, G. S., Stewart, G. R. & Williams R. S. "The missing memristor found," *Nature*, **453** (2008) pp. 80–83.
[10] Chua, L. O., "Memristor – The Missing Circuit Element," *IEEE Transactions on Circuit Theory* **18** (5) (1971) pp. 507–519.
[11] Ginoux, J.-M. & Rossetto, B., "The Singing Arc: The Oldest Memristor?" *Chaos, CNN, Memristors and Beyond*, in *Chaos, CNN, Memristors and Beyond: A Festschrift for Leon Chua*, World Scientific Publishing, Adamatsky, A. & Chen, G. (Eds) (2013) pp. 494–507.
[12] Muthuswamy, B. & Chua, L. O., "Simplest chaotic circuit," *International Journal of Bifurcation and Chaos*, 20(5) (2010) pp. 1567–1580.
[13] Di Garbo, A., Euzzor, S., Ginoux, J. M., Arecchi, F. T. & Meucci, R., "Delayed dynamics in an electronic relaxation oscillator," *Phys. Rev. E*, **100**, (2019) 032224.
[14] Björck, A., *Numerical Methods for Least Squares Problems*, SIAM, Philadelphia, pp. 407, 1996.
[15] Ginoux, J.-M., Meucci, R., Euzzor, S. & Di Garbo, A., "Torus Breakdown in a Uni Junction Memristor," *International Journal of Bifurcation and Chaos*, **28** (10), (2018) 1850128.
[16] Pugliese, E., Meucci, R., Euzzor, S., Freire, J.G. & Gallas, J.A.C., "Complex dynamics of a dc glow discharge tube: Experimental modeling and stability diagrams," *Sci. Rep.*, **5**, (2015) 08447.
[17] Lyapunov, A.M., *The General Problem of the Stability of Motion* (In Russian), Doctoral dissertation, Univ. Kharkov 1892, English translations: *The General Problem of the Stability of Motion*, (A. T. Fuller trans.) Taylor & Francis, London 1992, pp. 250.
[18] Sandri M., "Numerical Calculation of Lyapunov Exponents," *The Mathematica Journal*, **6**(3) (1996) pp. 78-84.

[19] Klein, M. & Baier, G., *Hierachies of dynamical systems*, In *A Chaotic Hierarchy*, edited by G. Baier and M. Klein. Singapore: World Scientific, 1991.
[20] Wolf, A., Swift, J.B., Swinney, H.L. & Vastano, J.A., "Determining Lyapunov Exponents from a Time Series," *Physica D*, **16** (1985) pp. 285-317.
[21] Eckmann, J.P. & Ruelle, D., "Ergodic Theory of Chaos and Strange Attractors," *Rev. Mod. Phys.*, **57** (1985) pp. 617-656.
[22] Hasegawa, Y., Tanaka, R. & Ueda, Y., "On Rational Phase-Locking Oscillations of a Simple Sawtooth Oscillator with UJT," *International Journal of Bifurcation and Chaos*, **11** (2001) pp. 3003–3032.
[23] Le Corbeiller, Ph., "Les Systèmes Auto-entretenus et les Oscillations de Relaxation," *Actualités scientifiques et industrielles*, vol. 144 (1931) Hermann, Paris.
[24] Poincaré, H., "Sur les courbes définies par une équation différentielle," *Journal de mathématiques pures et appliquées*, Série III **7**, (1881) pp. 375–422.
[25] Poincaré, H., "Sur les courbes définies par une équation différentielle," *Journal de mathématiques pures et appliquées*, Série IV **1**, (1885) pp. 167–244.
[26] Poincaré, H., "Sur les courbes définies par une équation différentielle," *Journal de mathématiques pures et appliquées*, Série IV **2**, (1886) pp. 151–217.
[27] Poincaré, H., *Les méthodes Nouvelles de la Mécanique Céleste*, Vol. I, II & III, Gauthier-Villars, Paris, 1892-93-99.